Journal of Sound and Vibration (1997) **200**(2), 179–194

USE OF THE ANALYTICAL-AND-NUMERICAL-COMBINED METHOD IN THE FREE VIBRATION ANALYSIS OF A RECTANGULAR PLATE WITH ANY NUMBER OF POINT MASSES AND TRANSLATIONAL SPRINGS

J.-S. Wu and S.-S. Luo

Institute of Naval Architecture and Marine Engineering, National Cheng-Kung University, Tainan, Taiwan 70101, *Republic of China*

(*Received* 20 *October* 1995, *and in final form* 11 *July* 1996)

By means of the analytical-and-numerical-combined method (ANCM), the natural frequencies and the corresponding mode shapes of a uniform rectangular flat plate carrying any number of point masses and translational springs are determined. The boundary (supported) conditions of the plate and the magnitudes and locations of the concentrated elements are arbitrary. First, the closed form solution of the natural frequencies and the normal mode shapes of the "unconstrained" plate (without any concentrated elements attached) are obtained. Second, based on the closed form solution and using the mode superposition technique, the eigenvalue equation of the "constrained" plate (with any number of concentrated elements attached) is derived. Finally, the eigenvalue equation is solved numerically to give the desired natural frequencies and mode shapes of the "constrained" plate.

Under the condition that the accuracies of the sought natural frequencies are approximately the same, the order of the eigenvalue equation derived from the ANCM is much lower than that derived from the traditional finite element method (FEM). Thus the CPU time required by the ANCM is much less than that required by the FEM.

Furthermore, the ANCM is also superior to the pure analytical (closed form solution) method, since the former (ANCM) is available for free vibration analysis of a uniform rectangular flat plate carrying any number of concentrated elements, but the latter is usually practical only for single concentrated elements.

1. INTRODUCTION

For convenience, a plate with prescribed boundary conditions without carrying any concentrated elements (such as point masses and/or translational springs) is called the "unconstrained" plate, and one carrying any number of concentrated elements is called the "constrained" plate in this paper. The analytical (closed form) solutions for the natural frequencies and mode shapes of a uniform "unconstrained" rectangular plate with various boundary conditions are easily obtained from the existing literature [1–4]. However, those of a uniform "constrained" rectangular plate are relatively fewer. For a uniform simply supported (all around) constrained rectangular plate carrying a concentrated mass, Gershgorin [1, 5] presented a closed form solution in 1933, and Amba-Rao [6] presented another closed form solution in 1964. Magrab [7] extended Amba-Rao's solution to include a plate simply supported on two opposite edges with the remaining two edges being simply supported, clamped or free, by using the combination of both the finite-sine transform and

0022–460X/97/070179 + 16 $25.00/0/sv960697

the Laplace transform in 1968. Shah and Datta [8] derived (1969) the analytical equations of motion of a rectangular constrained plate available for various boundary conditions. Although, the theory is valid for any number of point masses with moment of inertias, only the closed form solutions for the simple case of a concentrated mass with a moment of inertia are illustrated. In 1993, Ingber *et al*. [9] studied experimentally the vibration problem of a clamped (all around) rectangular plate with a spring–mass attachment by using a modal analysis technique, and numerically by using a mixed boundary – finite element method. For a thin rectangular plate having two opposite edges simply supported and with the other two edges being simply supported, clamped or free, Bergman *et al*. [10] presented (1993) a closed form solution for the plate with a central rigid support and that with an undamped single-degree-of-freedom linear oscillator.

It is obvious that all of the above-mentioned problems can be solved by the conventional finite element method (FEM) with little difficulty, but much more computing time is usually required. The analytical-and-numerical-combined method (ANCM) presented in this paper aims at avoiding the algebraic difficulties of the pure analytical method and the time-consuming nature of the FEM. The first author of the paper employed the ANCM for the first time to determine the natural frequencies and mode shapes of a uniform Euler beam carrying any number of point masses [11] in 1990, and then extended the theory to the free and forced vibration analyses of a Timoshenko beam with any number of translational and rotational springs and lumped masses with moment of inertias [12] in 1995. The problem presented in this paper is the third one that the first author has solved by using the ANCM. Instead of the half-interval method used in reference [11] and [12], the Jacobi method [13] is used to solve the eigenvalue problem in this paper, since the latter is more effective than the former for the present problem.

To demonstrate the effectiveness of the ANCM, the first five natural frequencies $\bar{\omega}_i (i = 1, \ldots, 5)$ of a uniform square plate (with dimensions $2\text{ m} \times 2\text{ m} \times 0{\cdot}005\text{ m}$) carrying a point mass (with a magnitude of 50 kg) are calculated by the ANCM and the FEM [14] and then compared with those calculated by exact solution [5, 6]. It is found that the accuracy of $\bar{\omega}_i (i = 1, \ldots, 5)$ obtained from the ANCM is much better than that obtained from the FEM. Additionally, the CPU time required by the ANCM is only 0·948% of that required by the FEM. Furthermore, to illustrate the application of the presented theory, the free vibration analysis of a rectangular plate ($2\text{ m} \times 3\text{ m} \times 0{\cdot}005\text{ m}$) carrying three concentrated masses (70, 50 and 60 kg) and three translational springs (with the spring constants 10^6, 10^4 and 10^5 N/m) located at the arbitrary positions and with four kinds of boundary conditions is made. It is found that the first five natural frequencies obtained from the ANCM are in good agreement with those obtained from the FEM, and the CPU time required by the ANCM is less than 2·31% of that required by the FEM for each boundary condition.

2. EQUATION OF MOTION AND ANALYTICAL SOLUTION FOR AN UNCONSTRAINED PLATE

By neglecting the effects of shear deformation and rotatory inertia, the equation of motion of a uniform rectangular unconstrained plate is given by [15]

$$D_E \nabla^4 w(x, y, t) + \rho \frac{\partial^2 w(x, y, t)}{\partial t^2} = p(x, y, t), \tag{1}$$

where $\nabla^4 = \partial^4/\partial x^4 + 2\partial^4/\partial x^2 \partial y^2 + \partial^4/\partial y^4$ is the biharmonic operator, $D_E = Eh^3/[12(1 - \nu^2)]$ is the flexural rigidity, E is the Young's modulus, h is the thickness, ν is the Poisson ratio,

ρ is the mass per unit area of the plate, $w(x, y, t)$ is the transverse deflection at position (x, y) and time t, and $p(x, y, t)$ is the transverse external loading.

Based on the mode superposition theory [16], the value of $w(x, y, t)$ due to forced vibration may be obtained from

$$w(x, y, t) = \sum_{i=1}^{n'} \bar{W}_i(x, y) q_i(t), \tag{2}$$

where $\bar{W}_i(x, y)$ is the ith "normal" mode shape of the "unconstrained" plate, $q_i(t)$ is the ith generalized co-ordinate, and n' is the mode number. For convenience of derivations, the normal mode shapes for a specified boundary condition may take various forms, but they must be arranged according to the magnitudes of the corresponding natural frequencies from the lowest mode to the higher modes. In other words, the corresponding natural frequency ω_i of $\bar{W}_i(x, y)$ must be in the order $\omega_1 < \omega_2 < \omega_3 < \ldots$.

Substituting equation (2) into equation (1), pre-multiplying both sides of the resulting equation by $\bar{W}_j(x, y)$, integrating the obtained expression over the area A of the plate and applying the orthogonality of the mode shapes, one obtains

$$\bar{M}_{jj}\ddot{q}_j(t) + \bar{K}_{jj} q_j(t) = \bar{P}_j(t), \qquad j = 1, \ldots, n', \tag{3}$$

where

$$\bar{M}_{jj} = \int_A \bar{W}_j \rho \bar{W}_j \, \mathrm{d}A, \qquad \bar{K}_{jj} = \int_A \bar{W}_j D_E \nabla^4 \bar{W}_j \, \mathrm{d}A, \qquad \bar{P}_j(t) = \int_A p(x, y, t) \bar{W}_j \, \mathrm{d}A \tag{4a–c}$$

represent the generalized mass, generalized stiffness and generalized force, respectively.

If $\bar{W}_j$ is a "normal" mode shape (with respect to ρ), then $\bar{M}_{jj} = 1{\cdot}0$, and equation (3) reduces to

$$\ddot{q}_j(t) + \omega_j^2 q_j(t) = \bar{P}_j(t), \qquad j = 1, \ldots, n', \tag{5}$$

where

$$\omega_j = \sqrt{\bar{K}_{jj}/\bar{M}_{jj}} = \sqrt{\bar{K}_{jj}} \tag{6}$$

is the jth natural frequency of the unconstrained plate. If the external load is a concentrated force with magnitude $\bar{P}$ and location (x_l, y_l), then equation (5) reduces to

$$\ddot{q}_j(t) + \omega_j^2 q_j(t) = \bar{P}(x_l, y_l, t) \bar{W}_j(x_l, y_l), \qquad j = 1, \ldots, n'. \tag{7}$$

3. EIGENVALUE EQUATION OF A CONSTRAINED PLATE

For a constrained plate performing free vibration, if the inertia forces of the concentrated masses and/or the restoring forces of the translational springs are considered the external exciting forces, then the forced vibration equation (7) for an "unconstrained" plate may be used to determine the natural frequencies and mode shapes of a "constrained" plate.

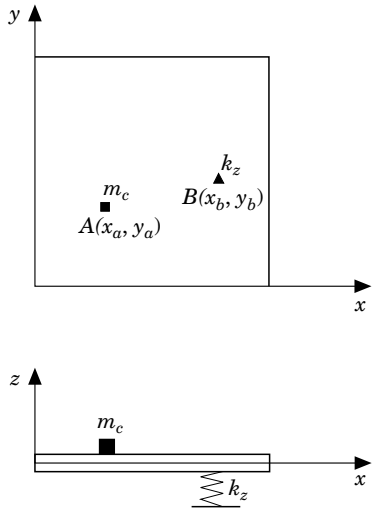

Figure 1. A rectangular plate carrying a concentrated mass m_c at point $A(x_a, y_a)$ and a translational spring k_z at point $B(x_b, y_b)$.

In Figure 1 is shown a rectangular plate carrying a concentrated mass m_c located at point $A(x_a, y_a)$ and a translational spring k_z located at point $B(x_b, y_b)$. The external forces on the plate during free vibration are given by

$$\bar{P}(x_a, y_a, t) = -m_c \frac{\partial^2 w(x_a, y_a, t)}{\partial t^2} = -m_c \sum_{i=1}^{n'} \frac{\partial^2 q_i(t)}{\partial t^2} \bar{W}_i(x_a, y_a), \tag{8a}$$

$$\bar{P}(x_b, y_b, t) = -k_z w(x_b, y_b, t) = -k_z \sum_{i=1}^{n'} \bar{W}_i(x_b, y_b) q_i(t), \tag{8b}$$

where m_c is the magnitude of the concentrated mass and k_z is the spring constant of the translational spring.

For a rectangular plate carrying p concentrated masses and q translational springs, from

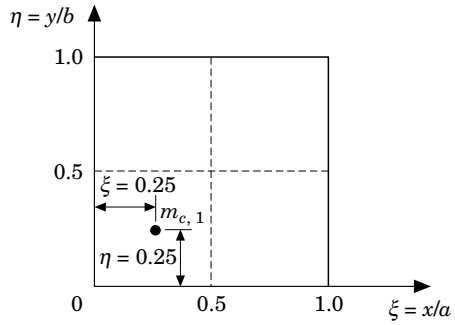

Figure 2. A uniform square plate carrying a concentrated mass $m_{c,1} = 50$ kg located at $\xi = 0{\cdot}25$ and $\eta = 0{\cdot}25$.

TABLE 1

The accuracy of FEM and ANCM and the CPU times required by each method

Method	Natural frequencies (rad/s) $\bar{\omega}_1$	$\bar{\omega}_2$	$\bar{\omega}_3$	$\bar{\omega}_4$	$\bar{\omega}_5$	CPU time (s)
Finite element method (FEM)	32·503 (2·130%)	63·913 (0·940%)	97·130 (1·797%)	130·077 (1·829%)	182·947 (1·262%)	633
Present method (ANCM)	31·814 (−0·034%)	63·232 (−0·136%)	95·415 (0.000%)	127·616 (−0·098%)	180·593 (−0·046%)	6 (0·948%)
Exact solution [5]	31·825	63·318	95·415	127·741	180·677	10 (1·50%)

equations (7) and (8) one obtains the following equations of motion of the "constrained" plate:

$$\ddot{q}_j(t) + \omega_j^2 q_j(t) = -\sum_{l=1}^{p} m_{c,l}\bar{W}_j(x_l, y_l)\sum_{i=1}^{n'}\bar{W}_i(x_l, y_l)\ddot{q}_i(t)$$

$$-\sum_{u=1}^{q} k_{z,u}\bar{W}_j(x_u, y_u)\sum_{i=1}^{n'}\bar{W}_i(x_u, y_u)q_i(t), \qquad j = 1, \ldots, n'. \tag{9}$$

When the constrained plate performing harmonic free vibration, the generalized co-ordinate $q_j(t)$ takes the form

$$q_j(t) = \bar{q}_j\, \mathrm{e}^{\mathrm{i}\bar{\omega}t}, \tag{10}$$

where $\bar{q}_j$ is the amplitude of $q_j(t)$ and $\bar{\omega}$ is the natural frequency of the constrained plate. The substitution of equation (10) into equation (9) yields

$$\omega_j^2\bar{q}_j + \sum_{u=1}^{q}\sum_{i=1}^{n'} k_{z,u}\bar{W}_j(x_u, y_u)\bar{W}_i(x_u, y_u)\bar{q}_i$$

$$= \bar{\omega}^2\bar{q}_j + \bar{\omega}^2\sum_{l=1}^{p}\sum_{i=1}^{n'} m_{c,l}\bar{W}_j(x_l, y_l)\bar{W}_i(x_l, y_l)\bar{q}_i \qquad j = 1, \ldots, n'. \tag{11}$$

Let

$$\{\bar{W}\}_{n'\times 1} = \{\bar{W}_1, \bar{W}_2, \ldots, \bar{W}_{n'}\}_{n'\times 1}, \qquad \{\bar{q}\}_{n'\times 1} = \{\bar{q}_1, \bar{q}_2, \ldots, \bar{q}_{n'}\}_{n'\times 1},$$

$$[\omega^2]_{n'\times n'} = \ulcorner\omega_1^2, \omega_2^2, \ldots, \omega_{n'}^2\lrcorner_{n'\times n'}, \qquad [I]_{n'\times n'} = \ulcorner 1, 1, \ldots, 1\lrcorner_{n'\times n'},$$

$$[\bar{W}]_{n'\times n'} = \{\bar{W}\}\{\bar{W}\}^{\mathrm{T}}, \qquad [A]_{n'\times n'} = \sum_{l=1}^{p} m_{c,l}[\bar{W}(x_l, y_l)], \qquad [B]_{n'\times n'} = \sum_{u=1}^{q} k_{z,u}[\bar{W}(x_u, y_u)], \tag{12}$$

then equation (11) may be rewritten as

$$[\omega^2]\{\bar{q}\} + [B]\{\bar{q}\} = \bar{\omega}^2([I] + [A])\{\bar{q}\} \tag{13}$$

or

$$[A']\{\bar{q}\} = \bar{\omega}^2[B']\{\bar{q}\}, \tag{14}$$

where

$$[A']_{n' \times n'} = [\ulcorner \omega^2 \urcorner] + [B], \qquad [B']_{n' \times n'} = [\ulcorner I \urcorner] + [A]. \tag{15}$$

In the above expressions, the symbols $\{\}$, $\ulcorner\ \urcorner$ and [] represent a column matrix, a diagonal matrix and a square matrix, respectively.

Equation (14) is the eigenvalue equation for a constrained plate. By means of the Jacobi method [13] one can obtain the eigenvalue $\bar{\omega}_j (j = 1, \ldots, n')$ and the eigenvector $\{\bar{q}\}^{(j)}$ $(j = 1, \ldots, n')$. It has been shown that $\bar{\omega}_j$ is the jth natural frequency of the "constrained" plate, and the corresponding natural mode shape $\tilde{w}_j(x, y)$ may be obtained from equation (2) and (10); i.e.,

$$\tilde{w}_j(x, y) = \sum_{i=1}^{n'} \bar{W}_i(x, y)\bar{q}_i^{(j)} = \{\bar{W}(x, y)\}^{\mathrm{T}}\{\bar{q}\}^{(j)}. \tag{16}$$

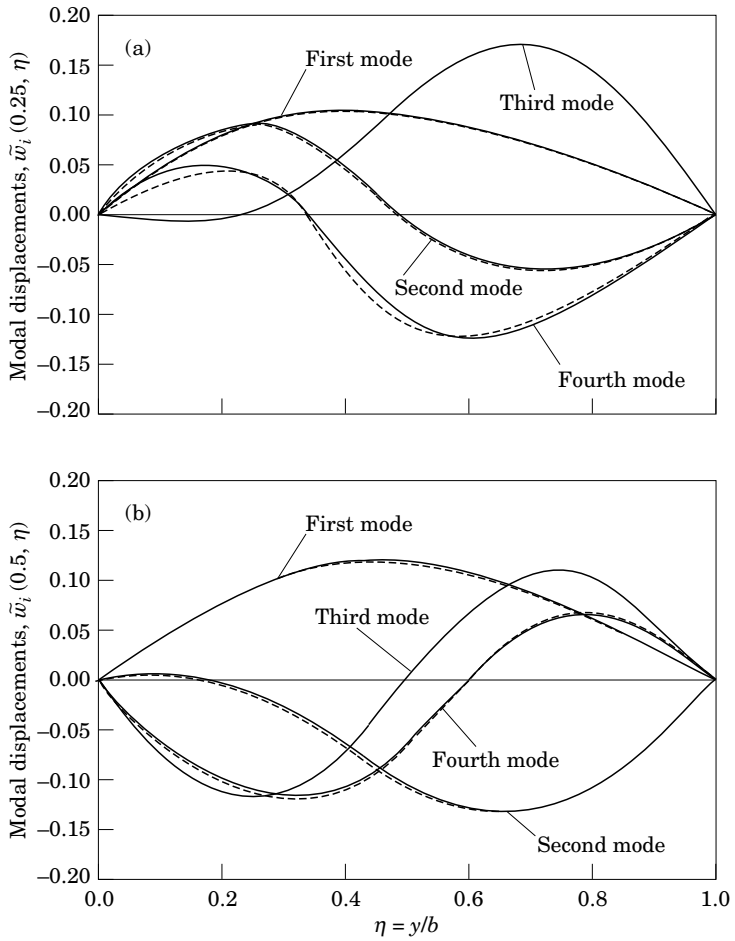

Figure 3. The first four mode shapes of the constrained square plate, $\tilde{w}_i(\xi, \eta)$, $i = 1, \ldots, 4$, located at (a) $\xi = 0{\cdot}25$ and (b) $\xi = 0{\cdot}5$, obtained from ANCM (——) and FEM (– – –).

TABLE 2

The influence of mode number (n') on the accuracy of $\bar{\omega}_i$ ($i = 1, \ldots, 5$) obtained from ANCM

Mode number n'	Natural frequencies (rad/s)				
	$\bar{\omega}_1$	$\bar{\omega}_2$	$\bar{\omega}_3$	$\bar{\omega}_4$	$\bar{\omega}_5$
5	32·09615 (0·853%)	65·69693 (3·757%)	95·41480 (0·000%)	131·8190 (3·192%)	186·57945 (3·267%)
10	31·92111 (0·303%)	64·10893 (1·249%)	95·41480 (0·000%)	128·89220 (0·901%)	181·43062 (0·417%)
15	31·90498 (0·252%)	63·97278 (1·034%)	95·41480 (0·000%)	128·68289 (0·737%)	181·28362 (0·336%)
20	31·86469 (0·126%)	63·64099 (0·510%)	95·41480 (0·000%)	128·20291 (0·361%)	180·97408 (0·165%)
25	31·82716 (0·003%)	63·33741 (0·030%)	95·41480 (0·000%)	127·76774 (0·021%)	180·69269 (0·009%)
30	31·81399 (−0·034%)	63·23190 (−0·136%)	95·41475 (−0·000%)	127·61601 (−0·098%)	180·59301 (−0·046%)
Exact solution	31·82478	63·31816	95·41495	127·74139	180·67666

4. NUMERICAL RESULTS AND DISCUSSION

4.1. RELIABILITY OF THE THEORY AND THE COMPUTER PROGRAM

To check the reliability of the present theory and the computer program developed for this paper, the first five natural frequencies and mode shapes of a uniform simply supported (SSSS) square plate carrying a concentrated mass $m_{c,1} = 50.0$ kg located at $\xi = x/a = 0{\cdot}25$ and $\eta = y/b = 0{\cdot}25$ as shown in Figure 2 are determined by using the present analytical-and-numerical-combined method (ANCM) and the conventional finite element method (FEM). Then, the two kinds of numerical (approximate) solutions are compared with the analytical (exact) solution [5], as shown in Appendix 2. The given data are: side length in x direction, $a = 2{\cdot}0$ m; side length in y direction, $b = 2{\cdot}0$ m; plate thickness, $h = 0{\cdot}005$ m; Young's modulus, $E = 2{\cdot}051 \times 10^{11}$ N/m^2; mass per unit area of plate, $\rho = 39{\cdot}25$ kg/m^2; Poisson ratio, $v = 0{\cdot}3$.

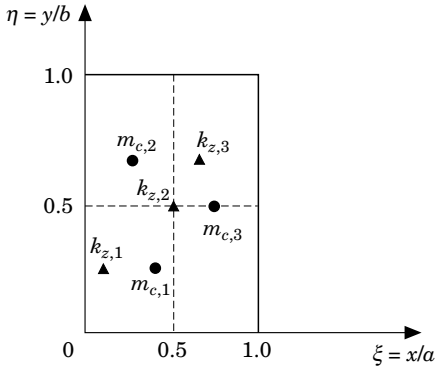

Figure 4. A uniform rectangular plate carrying three concentrated masses ($m_{c,1}$–$m_{c,3}$) and three translational springs ($k_{z,1}$–$k_{k,3}$).

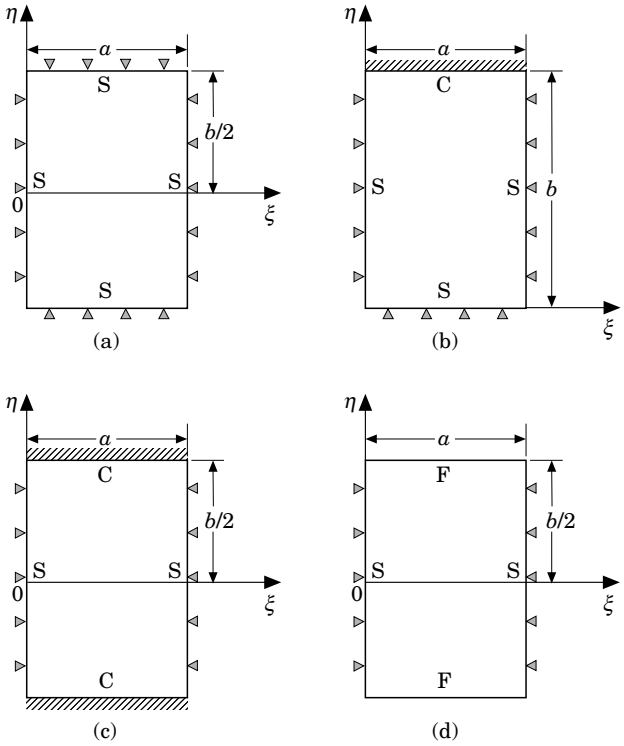

Figure 5. The four support conditions of the rectangular plate studied: (a) SSSS; (b) SSSC; (c) SCSC; (d) SFSF.

From the above-mentioned comparisons between ANCM, FEM and the exact solution [5], one finds that the accuracy of ANCM with 30 modes is approximately equal to that of the FEM with 64 plate elements. For this reason, the subsequent comparisons are based on the following criterion: the total number of plate elements for the FEM is 64 (the size of each element is $(a/8) \times (b/8)$, the total number of modes for the ANCM is 30, and that for the exact solution is 30 (i.e., $m = 6$, $n = 5$, $n' = m \times n = 30$). From Appendix 1 one sees that the degree of freedom for each plate element is $3 \times 4 = 12$ (as shown in Figure A1 below) and the element stiffness matrix $[K'^{(n)}]_c$ and the element mass matrix $[M'^{(n)}]_c$ for the "constrained" plate, as shown in equations (A4) and (A5), are the 12×12 square matrices.

Since the total number of modes taken by the ANCM or the exact solution is $n' = 30$, 30 natural frequencies and 30 mode shapes of the constrained square plate may be obtained. For simplicity, only the first five are shown in Table 1 and Figure 3. The figures in parentheses in the last column of Table 1 represent the percentage ratios of $(CPU)_{ANCM}$ or $(CPU)_{exact}$ to $(CPU)_{FEM}$, i.e., $(CPU)_m \times 100\%/(CPU)_{FEM}$, where $(CPU)_{ANCM}$, $(CPU)_{exact}$ and $(CPU)_{FEM}$ represent the CPU times required by the ANCM, the exact solution and FEM, respectively, and $m =$ ANCM or exact. The figures in the other parentheses in Table 1 represent the percentage errors between natural frequencies evaluated by the formula

$$\text{error} = [(\bar{\omega}_i - \bar{\omega}_{i,exact})/\bar{\omega}_{i,exact}] \times 100\%, \qquad i = 1, \ldots, n',$$

where $\bar{\omega}_i$ is the ith natural frequency obtained from ANCM or FEM. From Table 1 one sees that the accuracy of FEM is worse than that of ANCM, but the CPU time required by the FEM is more than 100 times of that required by the ANCM. The computer machine used is a Sun SPARC station.

Since the entire plate is composed of 64 elements (see Figure A1 below), the total degree of freedom for the simply supported (SSSS) plate is $(3 \times 81) - (2 \times 32) - 4 = 175$ and the overall stiffness matrix $[K]_c$ and the overall mass matrix $[M]_c$ appearing in equation (A6) are 175×175 square matrices. However, the matrices $[A']$ and $[B']$ defined by equation (15) and derived from the ANCM are the $n' \times n'$ $(=30 \times 30)$ ones. It is evident that $n' \ll 175$ is the main reason why the CPU time required by the ANCM is much less than that required by conventional FEM. Actually, a special-purpose computer program is used in this paper instead of the multi-purpose FEM computer package (software) and, therefore, the comparison of CPU times made in this paper should be fair. Additionally, for a thin plate the efficiency of the ANCM is not affected by factors such as the aspect ratio or the plate thickness.

In Figure 3 are shown the first four mode shapes $\tilde{w}_i(\xi, \eta)$ $(i = 1, \ldots, 4)$ located at $\xi = 0{\cdot}25$ and $\xi = 0{\cdot}5$, respectively. The solid lines represent the mode shapes obtained from the present method (ANCM) and the dashed lines represent those obtained from FEM. It is evident that they are in good agreement.

4.2. INFLUENCE OF MODE NUMBER (n') ON THE ACCURACY OF THE ANCM

In theory, equation (2) is correct only if the mode number n' approaches infinity (i.e., $n' \to \infty$) but, in practice, equation (2) will give satisfactory results by taking only a few modes. To realize the influence of the mode number n' on the accuracy of the natural frequencies of a constrained plate, the ones of the square plate shown in Figure 2 are calculated by means of the ANCM with mode number $n' = 5$, 10, 15, 20, 25 and 30, and then compared with the corresponding ones obtained from the exact solution [5] as shown in Table 2. The figures in parentheses in Table 2 represent the percentage errors between the natural frequencies obtained from the ANCM and those obtained from the exact solution. It can be seen that all of the percentage errors are less than 1·25% if the mode

TABLE 3

The first five natural frequencies of the constrained plate shown in Figure 4 *with the four support conditions shown in Figure* 5

Supported conditions	Methods	Natural frequencies (rad/s) $\bar{\omega}_1$	$\bar{\omega}_2$	$\bar{\omega}_3$	$\bar{\omega}_4$	$\bar{\omega}_5$	CPU time (s)
SSSS	FEM	28·831	39·775	47·158	82·898	105·352	633
	ANCM	28·632 (−0·690%)	39·392 (−0·963%)	48·084 (1·964%)	81·638 (−1·520%)	104·038 (−1·247%)	6 (0·948%)
SSSC	FEM	29·144	42·047	47·311	101·846	107·426	562
	ANCM	29·116 (−0·096%)	41·669 (−0·899%)	47·902 (1·249%)	99·826 (−1·983%)	105·447 (−1·842%)	9 (1·601%)
SCSC	FEM	31·461	43·880	48·664	102·370	120·807	433
	ANCM	31·409 (−0·165%)	43·502 (−0·861%)	49·290 (1·286%)	100·783 (−1·550%)	118·478 (−1·928%)	10 (2·309%)
SFSF	FEM	24·762	27·392	39·800	46·760	58·585	937
	ANCM	24·239 (−2·112%)	26·948 (−1·621%)	38·866 (−2·347%)	47·116 (0·761%)	58·588 (0·005%)	14 (1·494%)

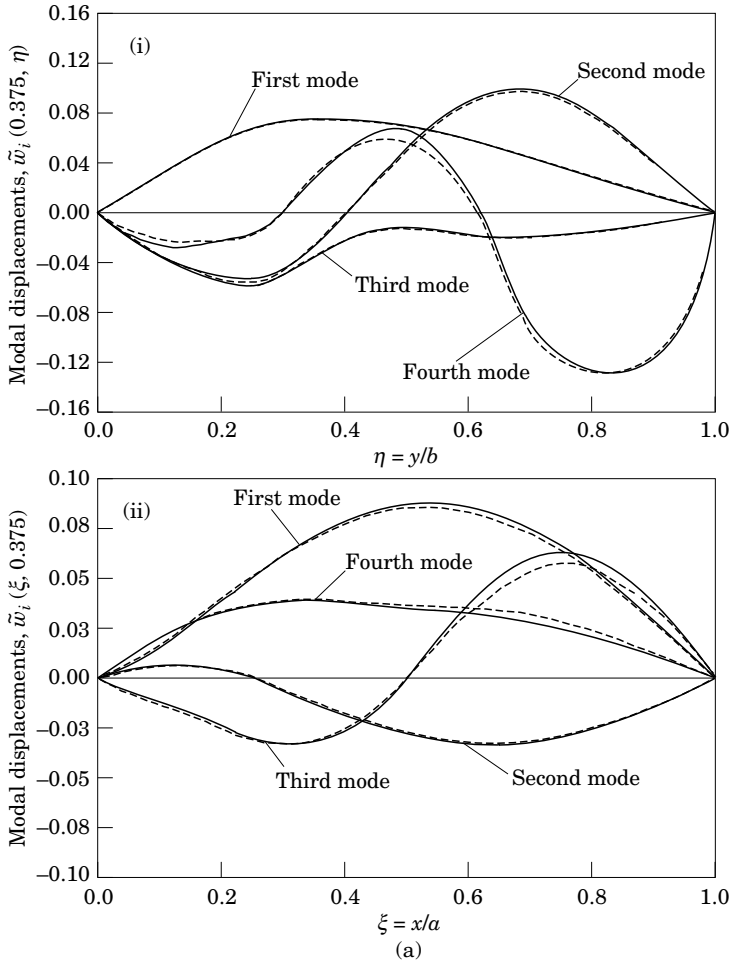

Figure 6—*caption on page* 191

number is larger than 10 (i.e., $n' \geqslant 10$). In fact, from the computer output one finds that the following conclusion drawn in references [11] and [12] is also valid for the present problem. Let n' be the mode number taken by the ANCM; then the accuracy of the lowest $n' - 1$ natural frequencies obtained will be acceptable.

4.3. A GENERAL CASE

In this section, the ANCM is used to calculate the first 30 natural frequencies $\bar{\omega}_i$ ($i = 1, \ldots, 30$) and the corresponding mode shapes $\tilde{W}_i(\xi, \eta)$ of a uniform rectangular plate carrying three concentrated masses $m_{c,l}$ ($l = 1, \ldots, 3$) and three translational springs $k_{z,u}$ ($u = 1, \ldots, 3$) (see Figure 4), to demonstrate the availability of the ANCM for a general constrained plate. The given data of the present example are: $a = 2{\cdot}0$ m, $b = 3{\cdot}0$ m, $h = 0{\cdot}005$ m, $E = 2{\cdot}051 \times 10^{11}$ N/m^2, $\rho = 39{\cdot}25$ kg/m^2, $\nu = 0{\cdot}3$, and

$$m_{c,1} = 70{\cdot}0 \text{ kg}, \quad \xi_{m,1} = 0{\cdot}375, \quad \eta_{m,1} = 0{\cdot}25,$$
$$m_{c,2} = 50{\cdot}0 \text{ kg}, \quad \xi_{m,2} = 0{\cdot}5, \quad \eta_{m,2} = 0{\cdot}625,$$
$$m_{c,3} = 60{\cdot}0 \text{ kg}, \quad \xi_{m,3} = 0{\cdot}75, \quad \eta_{m,3} = 0{\cdot}5,$$

$$k_{z,1} = 10^6 \text{ N/m}, \qquad \xi_{k,1} = 0{\cdot}125, \qquad \eta_{k,1} = 0{\cdot}25,$$
$$k_{z,2} = 10^4 \text{ N/m}, \qquad \xi_{k,2} = 0{\cdot}5, \qquad \eta_{k,2} = 0{\cdot}5,$$
$$k_{z,3} = 10^5 \text{ N/m}, \qquad \xi_{k,3} = 0{\cdot}625, \qquad \eta_{k,3} = 0{\cdot}625,$$

where $(\xi_{m,i}, \eta_{m,i})$ and $(\xi_{k,i}, \eta_{k,i})$ represent the locations (or co-ordinates) of the ith concentrated mass $m_{c,i}$ and the ith translational spring $k_{z,i}$, respectively.

Four support (boundary) conditions of the constrained plate are studied here. For convenience, a four-letter acronym is used to designate the type of support, starting at the left edge and proceeding in a counterclockwise direction. Hence, if the clamped, free and simply supported edges are denoted by C, F and S, respectively, then the boundary conditions of Figures 5(a)–(d) may be represented by SSSS, SSSC, SCSC and SFSF, respectively.

In Table 3 are shown the first five natural frequencies $\bar{\omega}_i$ $(i = 1, \ldots, 5)$ of the constrained plate shown in Figure 4 with the four supported conditions shown in Figure 5. In Figure 6(a)–(d) are shown the corresponding four transverse modal displacements for the four support conditions (a) SSSS, (b) SSSC, (c) SCSC and (d) SFSF; where (a)(i)–(d)(i)

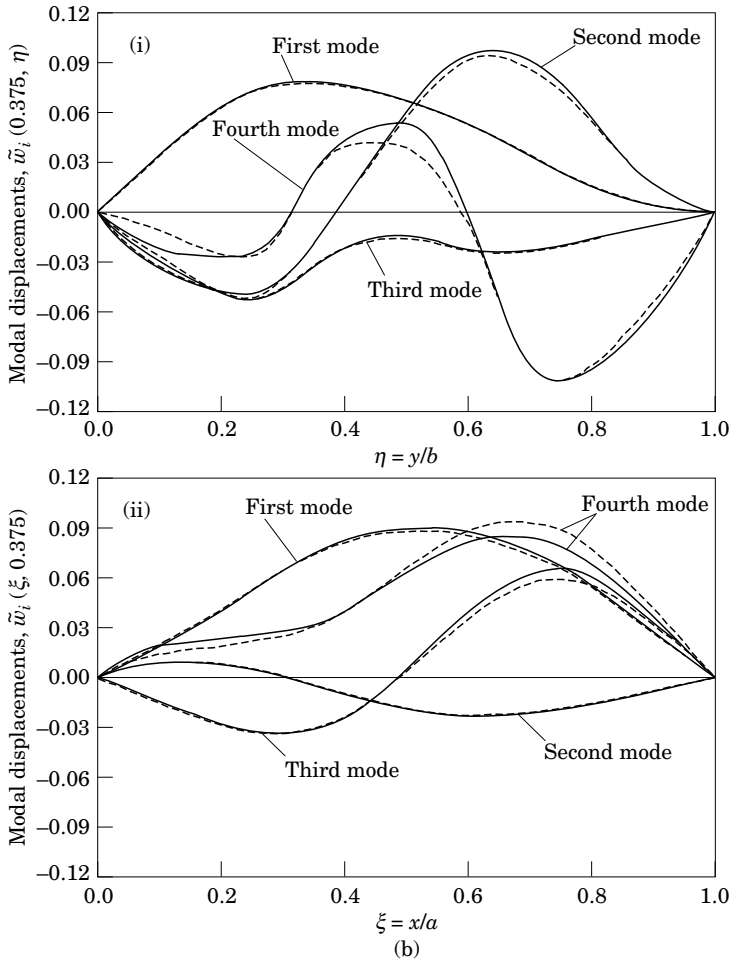

(b)

Figure 6—*caption on page* 191

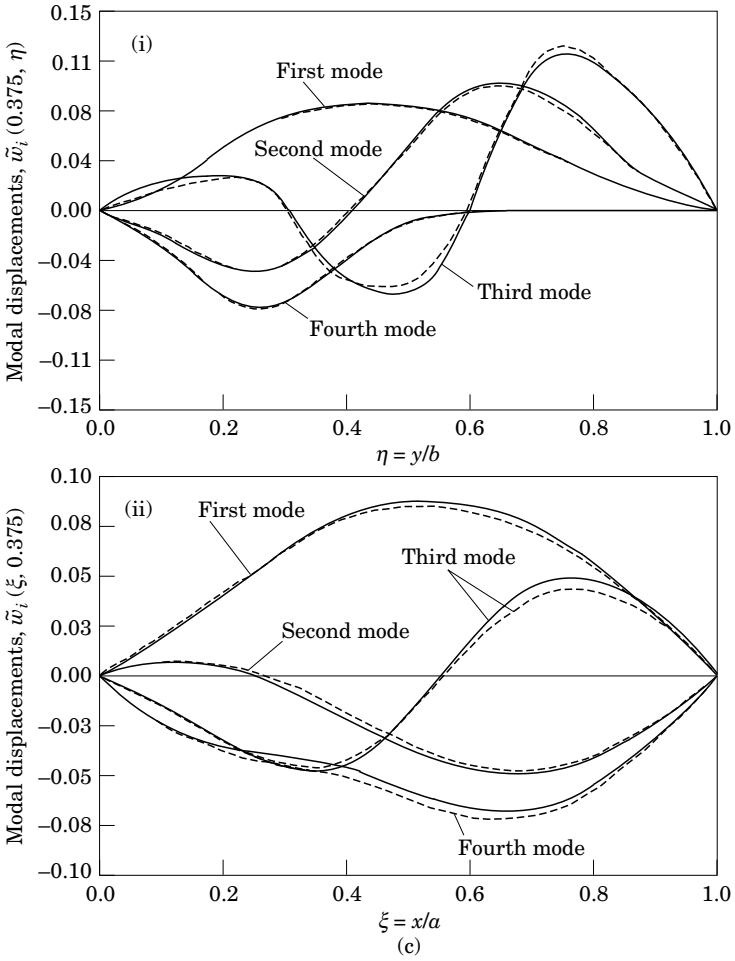

Figure 6—*caption opposite*

represent those located at $\xi = 0{\cdot}375$, i.e., $\tilde{w}_i(0{\cdot}375, \eta)$ and (a)(ii)–(d)(ii) represent those located at $\eta = 0{\cdot}375$, i.e., $\tilde{w}_i(\xi, 0{\cdot}375)$.

The figures (x) in parentheses of the last column in Table 3 represent the percentage ratios of the CPU times required by ANCM, $(CPU)_{ANCM}$, to those required by FEM, $(CPU)_{FEM}$, i.e., $(x\%) = (CPU)_{ANCM} \times 100\%/(CPU)_{FEM}$, and the figures ($y$) in the other parentheses in Table 3 represent the percentage "difference" between the natural frequencies obtained from ANCM, $\bar{\omega}_{i,ANCM}$, and those obtained from FEM, $\bar{\omega}_{i,FEM}$, i.e., $(y\%) = (\bar{\omega}_{i,ANCM} - \bar{\omega}_{i,FEM}) \times 100\%/\omega_{i,FEM}$. It is noted that percentage "difference" instead of percentage "error" is used here, since according to the foregoing analysis, the accuracy of ANCM may be better than that of FEM.

From Table 3 one can see that the values of $\bar{\omega}_{i,ANCM}$ are very close to those of $\bar{\omega}_{i,FEM}$ with a maximum difference less than 2·35%, and the maximum CPU time required by ANCM is less than 2·31% of that required by FEM. In other words, the ANCM can achieve accurate natural frequencies of a general constrained plate with various support conditions by consuming less than 2·31% of the CPU time required by the FEM.

From Figure 6 one can see that the first four mode shapes obtained from the present

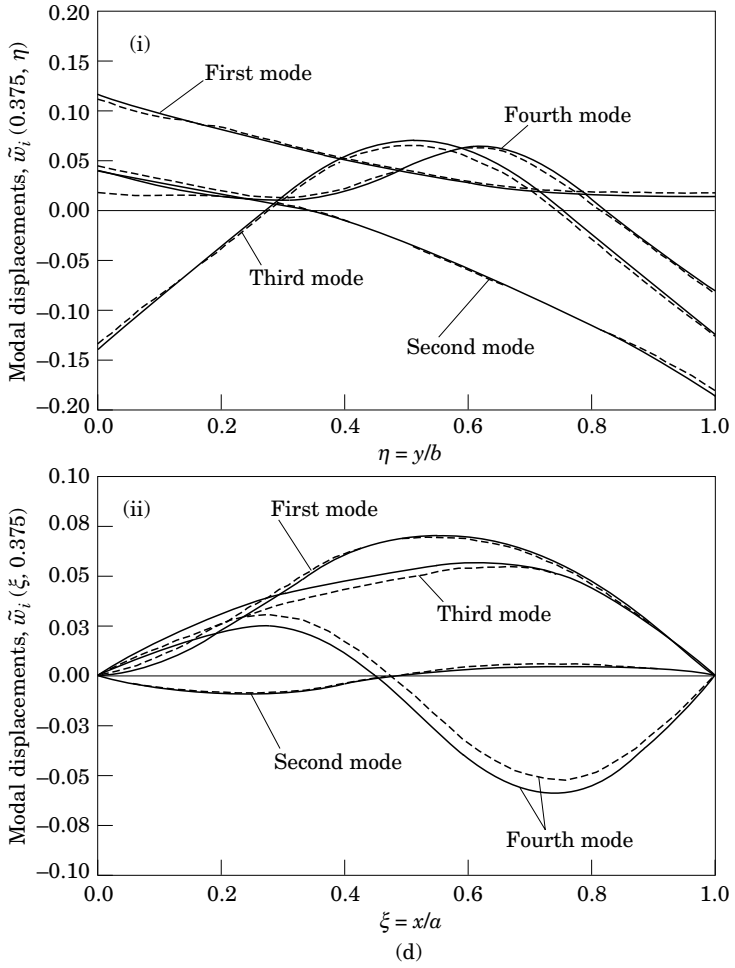

Figure 6. The first four transverse modal displacements $\tilde{w}_i(\xi, \eta)$ ($i = 1, \ldots, 4$) of the constrained rectangular plate obtained from ANCM (——) and FEM (– – – –) for the support conditions (a) SSSS, (b) SSSC, (c) SCSC and (d) SFSF, located at (i) $\xi = 0{\cdot}375$ and (ii) $\eta = 0{\cdot}375$, respectively.

method, ANCM (represented by the solid lines), are also very close to those obtained from the FEM (represented by the dashed lines).

5. CONCLUSIONS

1. For the case of approximately the same accuracy, the analytical-and-numerical-combined method (ANCM) presented in this paper determines the natural frequencies and mode shapes of a uniform rectangular plate carrying any number of concentrated elements with various support conditions by consuming only a few percent (e.g., less than 2·31%) of the CPU time required by the conventional finite element method (FEM).

2. If n' represents the total mode number taken by the ANCM, then the accuracy of the lowest $n' - 1$ natural frequencies of the constrained plate obtained from the ANCM will be acceptable.

3. Despite the fact that only four support conditions (SSSS, SSSC, SCSC and SFSF) for the "constrained" rectangular plate are studied in this paper, the ANCM is available

for the determination of the natural frequencies and mode shapes of the "constrained" plate with any other support conditions, the only requirement being that the closed form solution for the natural frequencies and normal mode shapes of the corresponding "unconstrained" plate is obtainable.

ACKNOWLEDGMENTS

The authors wish to acknowledge the financial support of the National Science Council of the Republic of China under contract No. NSC-85-2611-E-006-016.

REFERENCES

1. A. W. Leissa 1969 *Vibration of plates*. NASA SP-160.
2. A. W. Leissa 1973 *Journal of Sound and Vibration* **31**, 257–293. The free vibration of rectangular plates.
3. A. W. Leissa 1977 *The Shock and Vibration Digest* **9**, 13–24. Recent research in plate vibrations, part 1: classical theory.
4. D. J. Gorman 1982 *Free Vibration Analysis of Rectangular Plates*. New York: Elsevier North Holland.
5. S. Gershgorin 1933 *Prikl. Mat. Mekh.* **1**, 25–37. Vibrations of plates loaded by concentrated masses (in Russian).
6. C. L. Amba-Rao 1964 *Journal of Applied Mechanics* **31**, 550–551. On the vibration of a rectangular plate carrying a concentrated mass.
7. E. B. Magrab 1968 *Journal of Applied Mechanics* **35**, 411–412. Vibration of a rectangular plate carrying a concentrated mass.
8. A. H. Shah and S. K. Datta 1969 *Journal of Applied Mechanics* **36**, 130–131. Normal vibration of a rectangular plate with attached masses.
9. M. S. Ingber, A. L. Pate and J. M. Salazar 1992 *Journal of Sound and Vibration* **153**, 143–166. Vibration of a clamped plate with concentrated mass and spring attachments.
10. L. A. Bergman, J. K. Hall, G. G. G. Lueschen and D. M. McFarland 1993 *Journal of Sound and Vibration* **162**, 281–310. Dynamic Green's functions for Levy plates.
11. J. S. Wu and T. L. Lin 1990 *Journal of Sound and Vibration* **136**, 201–213. Free vibration analysis of a uniform cantilever beam with point masses by an analytical-and-numerical-combined method.
12. J. S. Wu and C. G. Huang 1995 *International Journal of Communications in Numerical Methods in Engineering* **11**, 743–756. Free and forced vibrations of a Timoshenko beam with any number of translational and rotational springs and lumped masses.
13. K. J. Bathe 1982 *Finite Element Procedures in Engineering Analysis*. Englewood Cliffs, NJ: Prentice-Hall.
14. J. S. Przemieniecki 1968 *Theory of Matrix Structural Analysis*. New York: McGraw-Hill.
15. R. Szilard 1972 *Theory and Analysis of Plates*. Englewood Cliffs, NJ: Prentice-Hall.
16. R. W. Clough and J. Penzien 1975 *Dynamics of Structures*. New York: McGraw-Hill.
17. L. Meirovitch 1967 *Analytical Method in Vibrations*. London: Macmillan.

APPENDIX 1: ELEMENT STIFFNESS MATRIX AND ELEMENT MASS MATRIX FOR THE "CONSTRAINED" RECTANGULAR PLATE

For a uniform "unconstrained" rectangular plate defined by equations (1)–(7), the corresponding finite element is shown in Figure A1, where u_z, θ_x, and θ_y are the element displacements at point (x, y), U_i $(i = 1, \ldots, 12)$ are the node displacements at the four nodes $(1, \ldots, 4)$, and a' and b' are the side lengths of the plate element in the x and y directions, respectively. If the relationship between u_z and $\{u\} = \{U_1 U_2 \ldots U_{12}\}$ is given by

$$u_z = [a_z]\{u\}, \tag{A1}$$

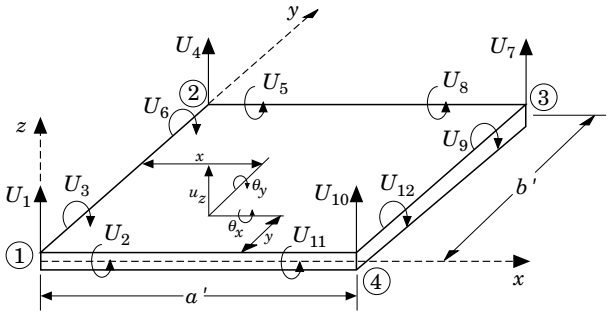

Figure A1. The element displacements (u_z, θ_x, θ_y) and node displacements U_i ($i = 1, \ldots, 12$) of a plate element.

then the stiffness matrix $[K']$ and the mass matrix $[M']$ of the plate element shown in Figure A1 may be obtained from [14]

$$[K'] = \int_V [B]^{\mathrm{T}}[D][B]\,\mathrm{d}V, \qquad [M'] = \int_V \rho[a_z]^{\mathrm{T}}[a_z]\,\mathrm{d}V \tag{A2, A3}$$

where $[B]$ is the strain–displacement matrix, $[D]$ is the elasticity matrix, $[a_z]$ is a row matrix composed of the shape functions, and V is the volume of the plate element.

The element stiffness matrix $[K']_c$ and mass matrix $[M']_c$ for the "constrained" plate are the same as those for the "unconstrained" plate defined by equations (A2) and (A3), the only difference being that the contributions of the translational springs $k_{z,u}$ ($u = 1, \ldots, q$) and the concentrated masses $m_{c,l}$ ($l = 1, \ldots, p$) must be added to the associated coefficients of the element stiffness matrices $[K']$ and the element mass matrices $[M']$, respectively. For example, if there exist a translational spring $k_{z,l}$ on the third node and a concentrated mass $m_{c,l}$ on the second node of the nth plate element (cf., Figure A1), then the stiffness matrix $[K'^{(n)}]_c$ and the mass matrix $[M'^{(n)}]_c$ of the nth plate element take the forms given below:

$$[K'^{(n)}]_c = \begin{bmatrix} K'^{(n)}_{1,1} & K'^{(n)}_{1,2} & \cdots & \cdots & \cdots & K'^{(n)}_{1,12} \\ K'^{(n)}_{2,1} & K'^{(n)}_{2,2} & & & & \vdots \\ \vdots & & \ddots & & & \vdots \\ \vdots & & & K'^{(n)}_{7,7} + k_{z,1} & & \vdots \\ \vdots & & & & \ddots & \vdots \\ K'^{(n)}_{12,1} & \cdots & \cdots & \cdots & \cdots & K'^{(n)}_{12,12} \end{bmatrix}_{12\times 12}, \tag{A4}$$

$$[M'^{(n)}]_c = \begin{bmatrix} M'^{(n)}_{1,1} & M'^{(n)}_{1,2} & \cdots & \cdots & \cdots & M'^{(n)}_{1,12} \\ M'^{(n)}_{2,1} & M'^{(n)}_{2,2} & & & & \vdots \\ \vdots & & \ddots & & & \vdots \\ \vdots & & & M'^{(n)}_{4,4} + m_{c,1} & & \vdots \\ \vdots & & & & \ddots & \vdots \\ M'^{(n)}_{12,1} & \cdots & \cdots & \cdots & \cdots & M'^{(n)}_{12,12} \end{bmatrix}_{12\times 12}, \tag{A5}$$

where the lower right subscript c for $[K'^{(n)}]$ and $[M'^{(n)}]$ refers to the property matrices of the "constrained" plate element.

Assembly of all element stiffness matrices and element mass matrices of the "constrained" plate will define the following eigenvalue equation:

$$([K]_c - \bar{\omega}_j^2[M]_c)\{\tilde{w}\}_j = 0, \qquad j = 1, \ldots, n'. \tag{A6}$$

By means of the Jacobi method [13], one may determine the natural frequencies $\bar{\omega}_j$ ($j = 1, \ldots, n'$) and the corresponding natural mode shapes $\{\tilde{w}\}_j$ of the "constrained" plate from equation (A6). In the last equation, $[K]_c$ and $[M]_c$ represent the overall stiffness matrix and the mass matrix of the "constrained" plate, respectively.

APPENDIX 2: EXACT SOLUTION FOR A UNIFORM RECTANGULAR PLATE CARRYING A POINT MASS

The equation of motion for a uniform rectangular plate carrying a concentrated mass m_c located at $x = u$ and $y = v$ is given by [6]

$$D_E\nabla^4 w(x, y, t) + [\rho + m_c\delta(x - u)\delta(y - v)]\frac{\partial^2 w(x, y, t)}{\partial t^2} = 0. \tag{A7}$$

If the side length in the x direction is a and that in the y direction is b, then the frequency equation for a SSSS plate is found to be [6]

$$1 = \frac{4m_c\bar{\omega}_{m,n}^2}{D_E ab}\sum_{m=1}^{\infty}\sum_{n=1}^{\infty}\left(\sin^2\frac{m\pi u}{a}\sin^2\frac{n\pi v}{b}\right)\Bigg/\left[\pi^4\left(\frac{m^2}{a^2} + \frac{n^2}{b^2}\right)^2 - \frac{\bar{\omega}_{m,n}^2}{D_E}\rho\right]. \tag{A8}$$

In this paper, the total mode number taken by the ANCM and the exact solution is $n' = m \times n = 30$; thus equation (A8) reduces to

$$\Delta(\bar{\omega}^2) = 1 - \frac{4m_c\bar{\omega}_{m,n}^2}{D_E ab}\sum_{m=1}^{6}\sum_{n=1}^{5}\left(\sin^2\frac{m\pi u}{a}\sin^2\frac{n\pi v}{b}\right)\Bigg/\left[\pi^4\left(\frac{m^2}{a^2} + \frac{n^2}{b^2}\right)^2 - \frac{\bar{\omega}_{m,n}^2}{D_E}\rho\right] = 0. \tag{A9}$$

From the last equation, one may determine the lowest 30 natural frequencies of the constrained rectangular plate, $\bar{\omega}_i$ ($i = 1, \ldots, 30$).